

Article

Characteristics and Formation Stages of Natural Fractures in the Fengcheng Formation of the Mahu Sag, China: Insights from Stable Carbon and Oxygen Isotope and Fluid Inclusion Analysis

Wei Wang¹, Xinhui Xie^{2,3,4,*}, Caiguang Liu¹, Feng Cao⁴, Guoqing Zheng¹, Zhenlin Wang¹, Gang Chen¹, Hucheng Deng⁴, Jianhua He⁴ and Kesai Li⁴

¹ PetroChina Xinjiang Oilfield Company, Karamay 834000, China; wangw_xj@petrochina.com.cn (W.W.); liucaiguang@petrochina.com.cn (C.L.); zgqxjyt@163.com (G.Z.); wzhenl@petrochina.com.cn (Z.W.); chenggang66@petrochina.com.cn (G.C.)

² Geophysics Post-Doctoral Station, Chengdu University of Technology, Chengdu 610059, China

³ College of Geophysics, Chengdu University of Technology, Chengdu 610059, China

⁴ College of Energy Resources, Chengdu University of Technology, Chengdu 610059, China; cf773992278@163.com (F.C.); denghucheng@cdut.cn (H.D.); hejianhua19@cdut.edu.cn (J.H.); l.k.s.2016@foxmail.com (K.L.)

* Correspondence: xxh0622@hotmail.com

Abstract: The Fengcheng Formation of the Mahu Sag is an unconventional reservoir that is of paramount importance for exploration and development of hydrocarbon resource. However, current research on natural fractures in the Fengcheng Formation remains limited, posing challenges for exploration of hydrocarbon resource in the region. This study is based on core observations, thin section identification, geochemical testing and the evolution of regional tectonic movements to investigate the characteristics and periods of formation of natural fractures to address this gap. According to the characteristics of natural fractures in the drilling core samples and microsections, the natural fractures in the Fengcheng Formation can be grouped into structural fractures and atectonic fractures. Structural fractures can be further divided into three subtypes: high-angle interlayer shear fractures, along-layer shear fractures, and tensile fractures. Additionally, non-tectonic fractures in this studied area are primarily bedding fractures, hydraulic fractures, and hydrocarbon-generating overpressure fractures. Vertically, fracture development is more prominent at the bottom of Feng #2 Formation and at the top of Feng #3 Formation. Results also indicate that natural fractures primarily formed during three distinct tectonic movement periods. The initial stage of fracture evolution pertains to the Late Permian period (243–266 Ma), filled with fibrous calcite, and exhibiting a uniform temperature of 70–100 °C. The second stage of fracture evolution occurred during the Late Indosinian to Early Yanshanian period (181–208 Ma), mostly filled or semi-filled with calcite, with a uniform temperature of 110–130 °C. The third stage of fracture development happened during the late Yanshanian to early Himalaya period (50–87 Ma), predominantly filled with calcite, and presenting a uniform temperature of 130–150 °C. Among the various types of structural fractures, the density of high-angle interlayer shear fractures demonstrates a positive correlation with daily gas production, indicating their vital role in promoting hydrocarbon resource production and transportation. Furthermore, microfractures generated by hydrocarbon-generating overpressure fractures exhibit small pore sizes and strong connectivity. These microfractures can create an effective permeability system by connecting previously isolated micropores in shale reservoirs, thus establishing interconnected pore spaces in the shale formation.

Keywords: natural fractures; fracture characteristics; formation stages of fractures; Fengcheng Formation; Mahu Sag



Citation: Wang, W.; Xie, X.; Liu, C.; Cao, F.; Zheng, G.; Wang, Z.; Chen, G.; Deng, H.; He, J.; Li, K. Characteristics and Formation Stages of Natural Fractures in the Fengcheng Formation of the Mahu Sag, China: Insights from Stable Carbon and Oxygen Isotope and Fluid Inclusion Analysis. *Minerals* **2023**, *13*, 894. <https://doi.org/10.3390/min13070894>

Academic Editor: Samintha Perera

Received: 5 May 2023

Revised: 8 June 2023

Accepted: 27 June 2023

Published: 30 June 2023



Copyright: © 2023 by the authors. Licensee MDPI, Basel, Switzerland. This article is an open access article distributed under the terms and conditions of the Creative Commons Attribution (CC BY) license (<https://creativecommons.org/licenses/by/4.0/>).

1. Introduction

The Junggar Basin in western China is an extensive and intricate sedimentary basin that has captivated the attention of geologists and petroleum exploration companies for numerous years. The Junggar Basin is renowned for its plentiful oil and gas reserves, which are predominantly concentrated in the Permian Fengcheng Formation situated within the Mahu Sag [1–3]. Prior studies propose that the oil and gas reserves in the Fengcheng Formation of the Mahu Sag could potentially reach up to 100 billion tons [4,5]. Natural fractures are crucial in the development of effective unconventional oil and gas reservoirs, as they function as storage spaces and permeable pathways for the flow of oil and gas [6,7]. In shale reservoirs, fractures exert a dual influence on the storage of oil and gas. Fractures, being weak structural planes, facilitate the formation of complex fracture networks during hydraulic fracturing [8]. Furthermore, fractures with high effectiveness can negatively impact storage space, potentially resulting in oil and gas leakage [9]. Therefore, it is essential to investigate the basic characteristics and formation periods of natural fractures for shale oil and gas exploration and development. This study can provide an accurate geological foundation for subsequent oil and gas reservoir deployment, development plan formulation, and optimization [10–12].

The Mahu Sag of the Junggar Basin is a promising exploration area for organic-rich shale formations, particularly the Fengcheng Formation [3,13]. The Fengcheng Formation has experienced multiple tectonic movements, which makes it challenging to determine the periods of fracture formation based solely on outcrop and core observations [4,14–16]. To date, the fluid inclusion test and stable carbon and oxygen isotope analysis of filling materials in the fractures can be regarded as effective and feasible methods for determining the evolution of fracture formation [17–19]. The fractures in the Fengcheng Formation are subjected to various stresses, including regional tectonic compression and shear slip. These stresses result in the development of complex fracture systems. Therefore, it is essential to examine the characteristics and formation period evolution of natural fractures of different origins in the studied area to clarify the favorable exploration area for shale oil and gas [10,15,17].

This study aims to examine the characteristics and formation stages of natural fractures in the Fengcheng Formation of the Mahu Sag using a diverse range of methods, including drill core analysis, thin section petrography, image logging, fluid inclusion testing, and carbon and oxygen isotope analysis. Initially, natural fractures are classified into two main types and six subtypes based on their mechanical origin. Moreover, the evolution of natural fractures throughout the formation period is analyzed by scrutinizing the crosscutting relationships among different fracture groups and interpreting geochemical findings. Subsequently, we also discuss the influence of various fracture types on oil productivity. By elucidating the interrelated dynamics between multistage fractures, this research can provide a geological foundation for shale reservoir exploration in the Mahu Sag.

2. Geological Setting

Figure 1 shows the structural zone and well locations of the Mahu Sag in the Junggar Basin. In this study, shale samples obtained from eleven wells in the Mahu Sag are used to survey the natural fracture characteristics. As one of the six primary hydrocarbon-rich depressions in the Junggar Basin, it occupies an exploration area of approximately 1×10^4 km² [20–22]. The Mahu Sag is a foreland basin formed by compression between the Kazakhstan Plate and the West Junggar Ocean. This region is distinguished by a significant depression of hydrocarbon-rich resources.

The northern region of the Mahu Sag has experienced multiple tectonic events, including Hercynian, Indosinian, Yanshanian, and Himalayan movements. These Yanshanian and Himalayan events led to the region's overall elevation, yielding a relatively comprehensive stratigraphy. The stratigraphy of the Mahu Sag, from the top to the bottom, comprises Quaternary, Neogene, Paleogene, Cretaceous, Jurassic, Triassic, Permian, and Carboniferous [23]. The Fengcheng Formation in the Permian is the focus in this study,

which constitutes a crucial source rock. The Fengcheng Formation composed of mudstone, marl, siltstone, mudstone sandstone, and mudstone fine sandstone, which can be classified into three sections based on sedimentary and lithofacies characteristics: Fengcheng #3 Formation (P_{1f3}), Fengcheng #2 Formation (P_{1f2}), and Fengcheng #1 Formation (P_{1f1}). On the plane, a northwest-thick and southeast-thin trend is discernible, leading to a thinning trend from northwest to southeast in each section of the Fengcheng Formation.

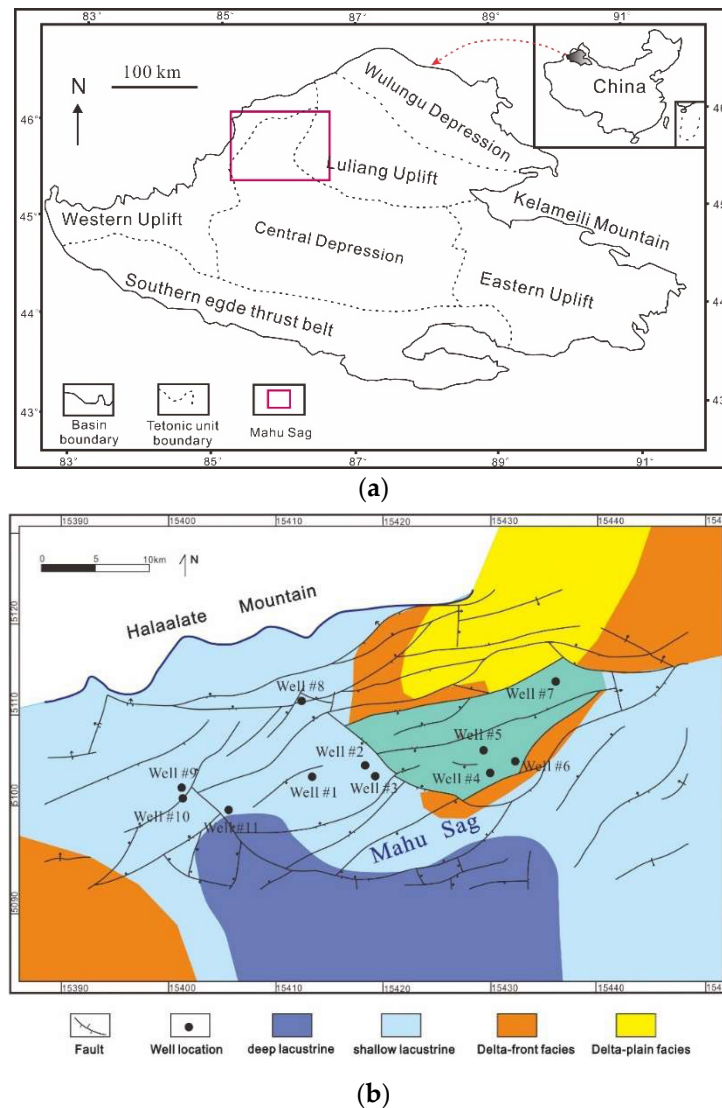


Figure 1. (a) The relative location of the studied areas in Junggar Basin, and (b) well locations of shale samples in the Mahu Sag of the Junggar Basin.

3. Methodologies

3.1. Drilling Core and Micro-Section Observation

A total of 35 micro-sections from 10 drilling wells are applied to analyze the microscope of samples. To facilitate pore volume identification, blue dye resin is introduced into the thin sections, while a combination of Alizarin Red-S and potassium ferricyanide is employed to assist in discerning carbonate minerals. Then, a polarizing microscope can be utilized to determine the mineral composition, texture, and validity of pores and fractures.

3.2. Borehole Image Logs

Borehole image logs can provide valuable insights into fracture characteristics, sedimentary structures, geomechanical properties, and depositional trends. Advances in

imaging technology have significantly improved the visualization of these features, particularly in non-cored intervals. To evaluate fracture strikes, image log (FMI) data from both cored and non-cored sections are employed, offering a comprehensive understanding of the subsurface fracture patterns. Incorporating FMI data into the analysis allows for a more complete and detailed understanding of the fracture network within the Fengcheng Formation of the Mahu Sag.

3.3. Fluid Inclusion Test

During mineral crystallization, fluid inclusions become entrapped in defects or voids within the mineral lattice. These inclusions are preserved inside the primary mineral. Determining the temperature of primary inclusions that formed simultaneously with the fracture fillings is a commonly accepted method for estimating the period of fracture formation. By assessing the temperature of primary inclusions that formed concurrently with the fracture fillings, the timeframe of fracture formation can be estimated.

3.4. Stable Carbon and Oxygen Isotope Analysis

The sample containing the fracture fill is subjected to reaction with 100% orthophosphoric acid at a constant temperature, resulting in the production of carbon dioxide and water. The carbon dioxide is purified and the isotopic composition of $\delta^{13}\text{C}$ and $\delta^{18}\text{O}$ is measured using a gas isotope mass spectrometer, with the precision exceeding $\pm 0.2\%$. The experimental apparatus is fDeltaV isotope ratio mass spectrometer.

3.5. Nano-CT Tests

The NanoCT scanner (MicroXRM-L200, ZEISS, Oberkochen, Germany) is used to analyze the distribution characteristics of pores, fractures and grains in a sample. The scanner employs a constant X-ray source voltage of 40 kV with a photon energy of 8 keV. Before testing, the sample should be cut into approximately cylindrical shapes with a diameter of about 100 μm . The scanner has a high resolution in scanning mode, with a large field of view that allows for a visual field of 65 μm and a resolution of 65 nm.

3.6. FE-SEM Experiment

The SEM experiment (Quanta 250 FEG, Thermo Fisher, Waltham, MA, USA) is utilized to determine the microfracture characteristics of shale samples. The experiment is conducted in a highly-vacuumed environment, and images are captured at a magnification ratio ranging from 6 to 1,000,000. Prior to FE-SEM analysis, the samples are coated with a layer of gold and polished using an argon-ion polishing system (Gatan 685, Gatan, Pleasanton, CA, USA).

4. Results and Discussion

4.1. Fracture Characteristics

Natural fractures in the Fengcheng Formation of the Mahu Sag are characterized by the observation of drilling cores and imaging logging images. Specifically, downhole shale samples from five wells and imaging logging images from eight wells are utilized to survey the natural fracture characteristics in the area. Figure 2 depicts the characteristics of the natural fractures in the Fengcheng Formation of the Mahu Sag. Results indicate that the length of the fractures in the Fengcheng Formation falls in the range from 5 cm to 15 cm, with over 85% of the fractures exceeding 5 m in length. The fracture width spans 0.1 mm–2 mm, with the majority falling between 0.2 mm to 1 mm. The inclination angle of the fractures is mostly medium to high, with more than 71% having an angle greater than 60° . Furthermore, approximately 78% of the natural fractures are filled with calcite, quartz, dolomite, and asphalt, with calcite as the principal filling mineral (Figure 2).

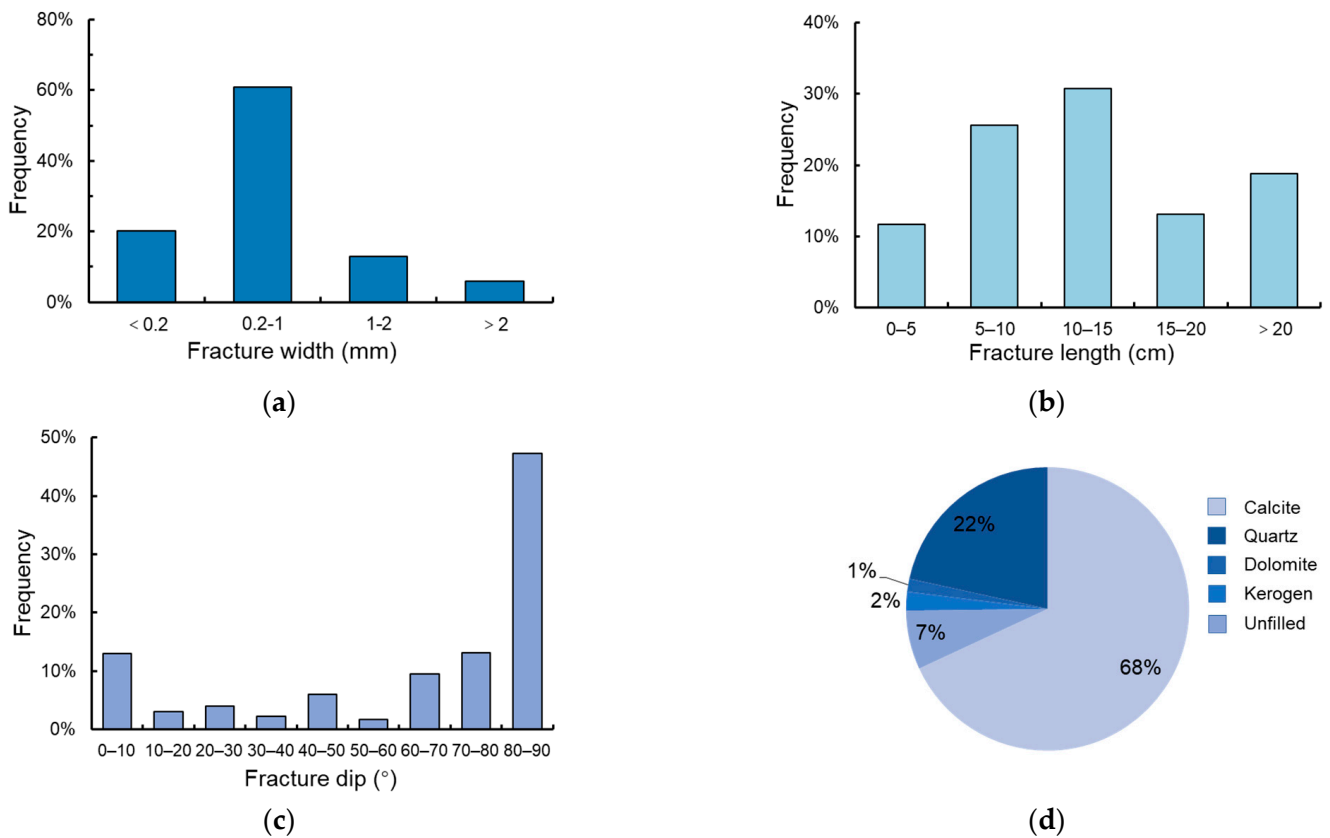


Figure 2. The statistical results of fracture characteristics and fillings of fractures from the drilling cores, microsections, and borehole imaging logging data. (a) Frequency distribution of fracture widths in the study area; (b) Frequency distribution of fracture lengths in the study area; (c) Frequency distribution of fracture dips in the study area; (d) Map of the percentage of fracture fills in the study area.

Figure 3 displays a detailed column chart of the fractures profile for Well #3 in the Fengcheng Formation of the Mahu Sag. The results reveal that the distribution of natural fractures in the Fengcheng Formation of the Mahu Sag is relatively uniform. The density of natural fractures decreases progressively with depth. The Feng #3 Formation displays the highest fracture density, spanning from 5 pcs/m to 75 pcs/m with an average value of 14.52 pcs/m. The Feng #2 Formation has a fracture density of 3 pcs/m to 58 pcs/m (average at 25.29 pcs/m), while the Feng #1 Formation exhibits the lowest fracture density, ranging from 3 pcs/m to 10 pcs/m (average at 8.56 pcs/m). The bottom of Feng #2 Formation and the top of Feng #3 Formation demonstrate the most significant degree of fracture development. The degree of fracture development in the Fengcheng Formation of the Mahu Sag appears to be influenced by the mineral composition of the shale samples. Specifically, fracture densities within the shale formation exhibit a positive correlation with increasing brittle mineral content. Shale formations with higher concentrations of brittle minerals (i.e., quartz, feldspar, calcite and dolomite) appear to be more prone to the generation of fractures [22].

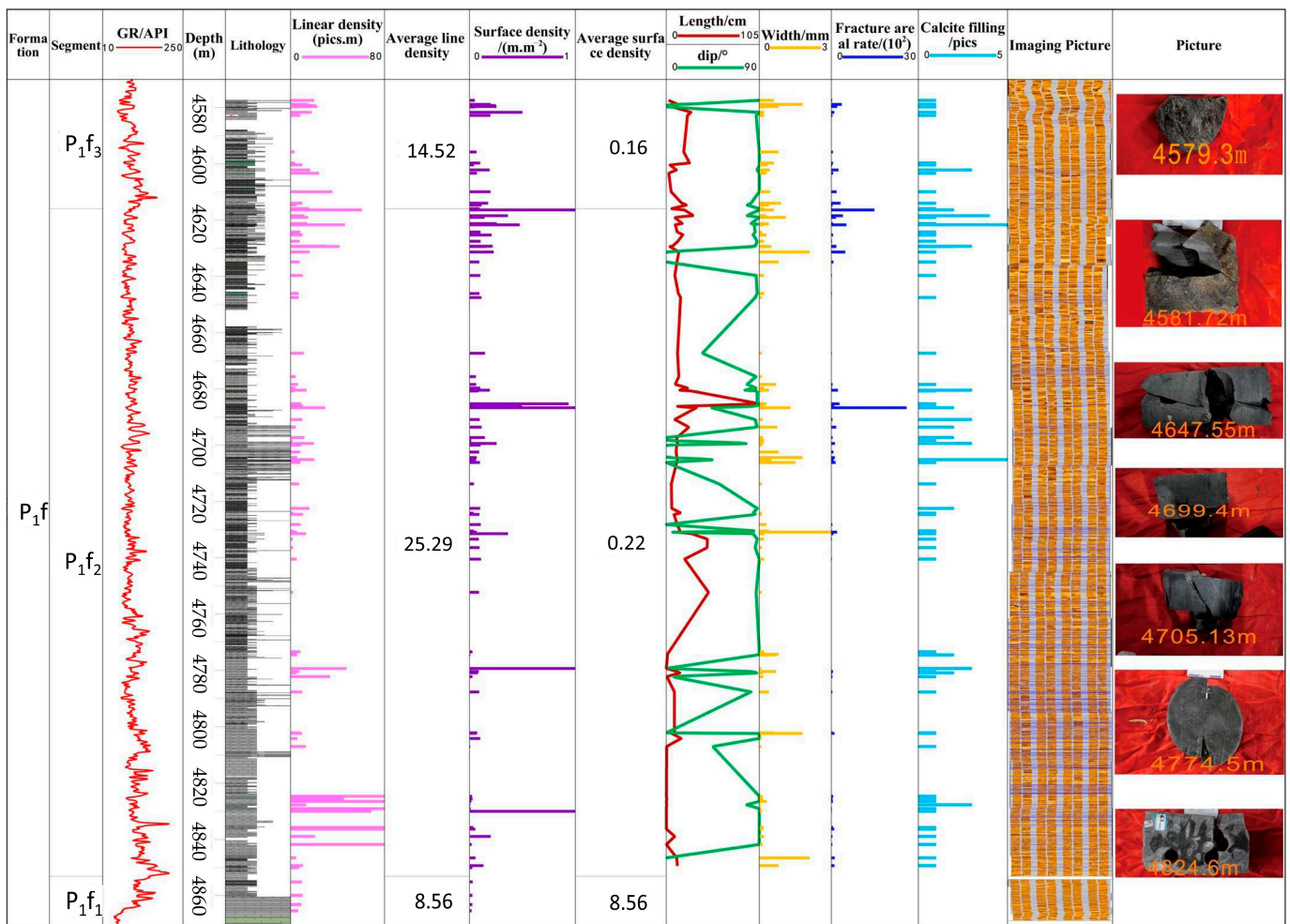


Figure 3. The column chart of the fracture profile for Well #3 in the Fengcheng Formation of the Mahu Sag.

4.2. The Classification of Fractures Based on Mechanical Origin

Based on observations of drilling core samples and microsections, the fractures in the Fengcheng Formation can be divided into two types: structural fractures and atectonic fractures. Structural fractures are primarily controlled by tectonic compression. The Mahu Sag, having experienced multiple episodes of intense tectonic activity, exhibits a complex structural fracture characteristic. Based on mechanical properties, the tectonic fractures in the Fengcheng Formation of the Mahu Sag can be further divided into three subtypes: high-angle interlayer shear fractures, along-layer shear fractures, and tensile fractures. Figure 4 demonstrates core sample photos and microsections of samples that contain tectonic fractures. The high-angle interlayer shear fractures depicted in Figure 4a–c exhibit straight and uniform fracture surfaces. Interactions between distinct sets of interlayer shear fractures involve mutual cutting and constraint. These types of fractures display a conjugated shear distribution filled with calcite and quartz. Generally, interlayer shear fractures are commonly developed in shale formations, which are abundant in brittle minerals. Along-layer slip shear fractures are characterized by distinctive features, including striations, mirror-like surfaces, and step-like structures with low-dip angles (Figure 4d,e). These fractures emerge in the context of tectonic stresses generated by compressional or extensional forces. Figure 4f depicts microsections of shale samples from Well #3, demonstrating the validity of along-layer slip shear fractures within the sample. Tensile fractures, formed in the condition of tensile stresses, are characterized by limited and unstable extension lengths. The widths of tensile fractures are variable, with rough and uneven fracture surfaces. Furthermore,

the extension direction of tensile fractures typically aligns parallel to the primary stress direction (Figure 4g,h). Additionally, these types of fractures observed in thin sections are mostly unfilled with mineral (Figure 4i).

Non-tectonic fractures in the Fengcheng Formation of the Mahu Sag are primarily bedding fractures, hydraulic fractures, and hydrocarbon-generating overpressure fractures. Bedding fractures are characterized by near-horizontal or low-angle features, exhibiting rough surfaces (Figure 4j). In the microscope, the bedding fractures appear parallel to each other and display a wavy pattern (Figure 4h,i). Hydraulic fractures, typically filled with fibrous calcite, possess restricted extension lengths. The fracture surface manifests discernible branching configurations, evocative of tree branches (Figure 4m–o). The majority of fractures generated by hydrocarbon-generating overpressure fractures are microscopic fractures that exhibit high effectiveness. Based on the microsection and FE-SEM images, these types of fractures mostly occur at the edges of mineral grains or inside organic matter with irregular shapes (Figure 4p–r).

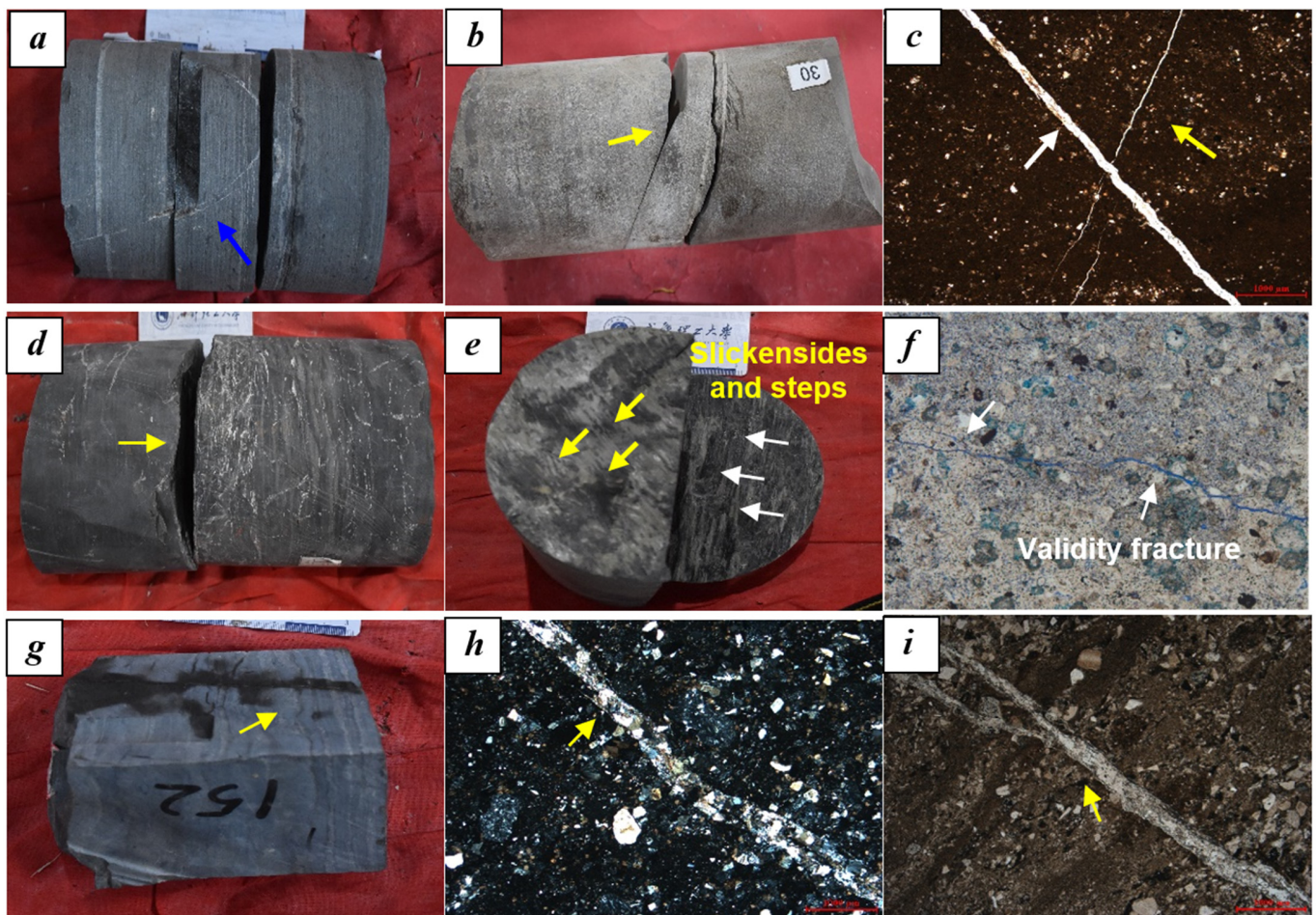


Figure 4. Cont.

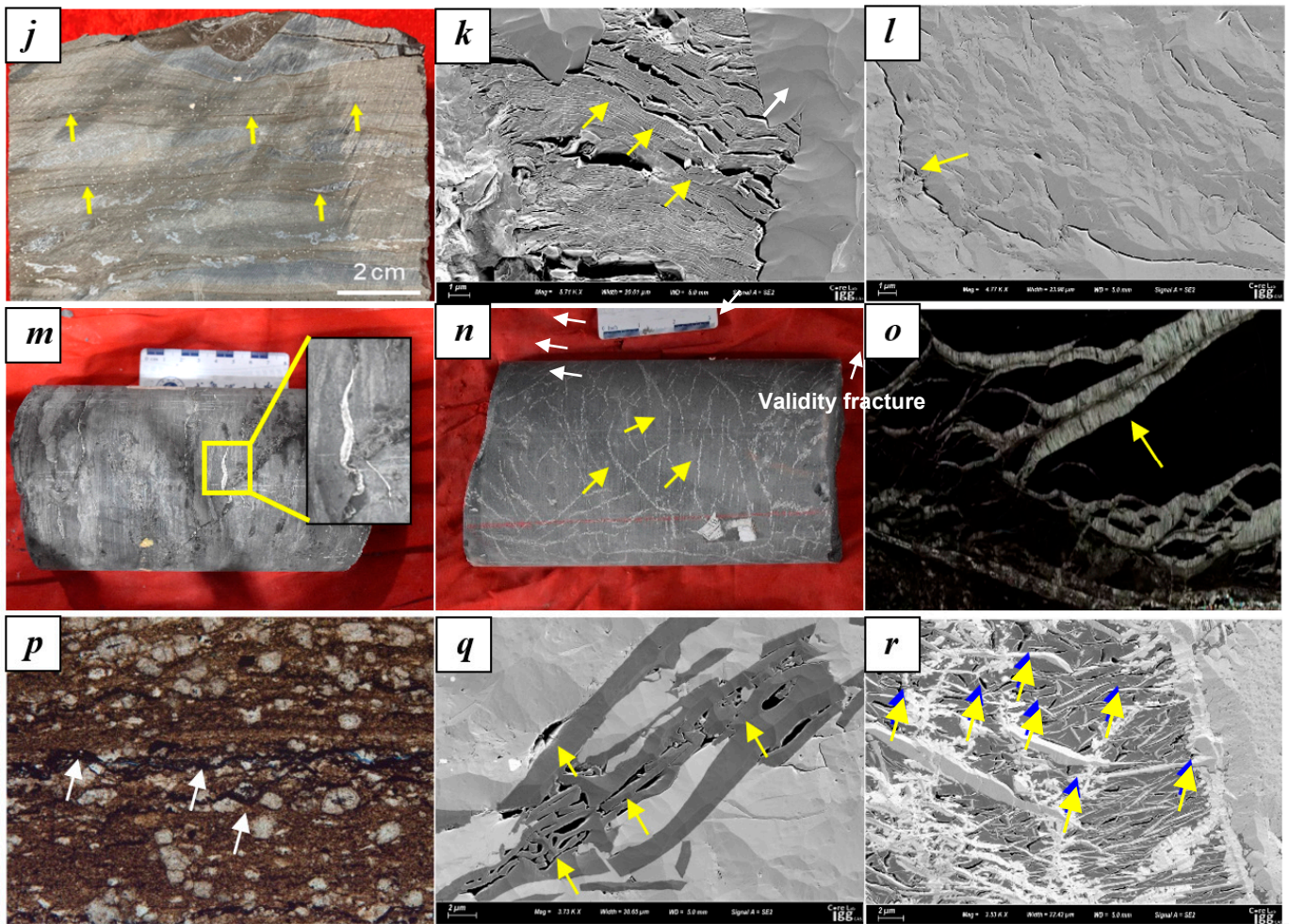


Figure 4. The drilling cores, microsections and FE-SEM images showing the different types of fractures of Fengcheng Formation in the Mahu Sag of the Junggar Basin, China. (a) The high-angle interlayer shear fracture with calcite filling, Well #6, 4744.48 m; (b) The unfilled high-angle interlayer shear fracture, Well #1, 4744.48 m; (c) Straight and uniform high-angle interlayer shear fracture with calcite filling, Well #6, 4647.30 m; (d) The unfilled along-layer -shear fracture, Well #6, 4648.10 m; (e) Along-layer-shear fracture with step-like structures with low-dip angle, Well #3, 4697.32 m; (f) The unfilled along-layer slip shear fracture, Well #3, 4636.14 m; (g) Tensile fractures unfilled, Well #3, 4627.53 m; (h) Tensile fractures with calcite filling, Well #3, 4614.20 m; (i) The unfilled tensile fractures, Well #3, 4616.41 m; (j) low-angle bedding fractures, Well #1, 4061.60 m; (k) The bedding fractures in the microscope, Well #3, 4740.43 m; (l) The unfilled bedding fractures, Well #3, 4802.20 m; (m) Hydraulic fractures filled with fibrous calcite, Well #6, 4640.47 m; (n) Hydraulic fractures with discernible branching configurations in the fracture surface, Well #6, 4668.90 m; (o) Hydraulic fractures in the microscope, Well #3, 4664.85 m; (p) Hydrocarbon-generating overpressure fractures with kerogen filling, Well #3, 4744.48 m; (q) The unfilled hydrocarbon-generating overpressure fractures, Well #3, 4802.20 m; (r) The unfilled Hydrocarbon-generating overpressure fractures, Well #3, 4759.42 m.

4.3. Comprehensive Determination of the Evolution Periods of Fractures

A total of seventeen shale samples were utilized to explore the evolution periods of fractures based on the cutting relationship of natural fractures on the macro- and micro-scales, fluid inclusion test, and stable carbon and oxygen isotope analysis.

4.3.1. The Observation of Drilling Cores and Microsections

The formation periods of natural fractures can be inferred by examining the filling order and intersection relationships among different fractures on core samples. Figure 5a–c

display two sets or three sets of shear fractures, which were filled with calcite. In Figure 5a, a late-formed high-angle cross-layer shear fracture is observed cutting through two early-formed cross-layer shear fractures. Figure 5b shows a late-formed high-angle tensile fracture intersecting with an early-formed bedding fracture. Figure 5c illustrates a late-formed shear fracture passing through an unfilled bedding fracture and an earlier-formed calcite-filled bedding fracture. Figure 5d depicts a rose diagram of strikes of tectonic fractures, indicating three formation periods of natural fractures.

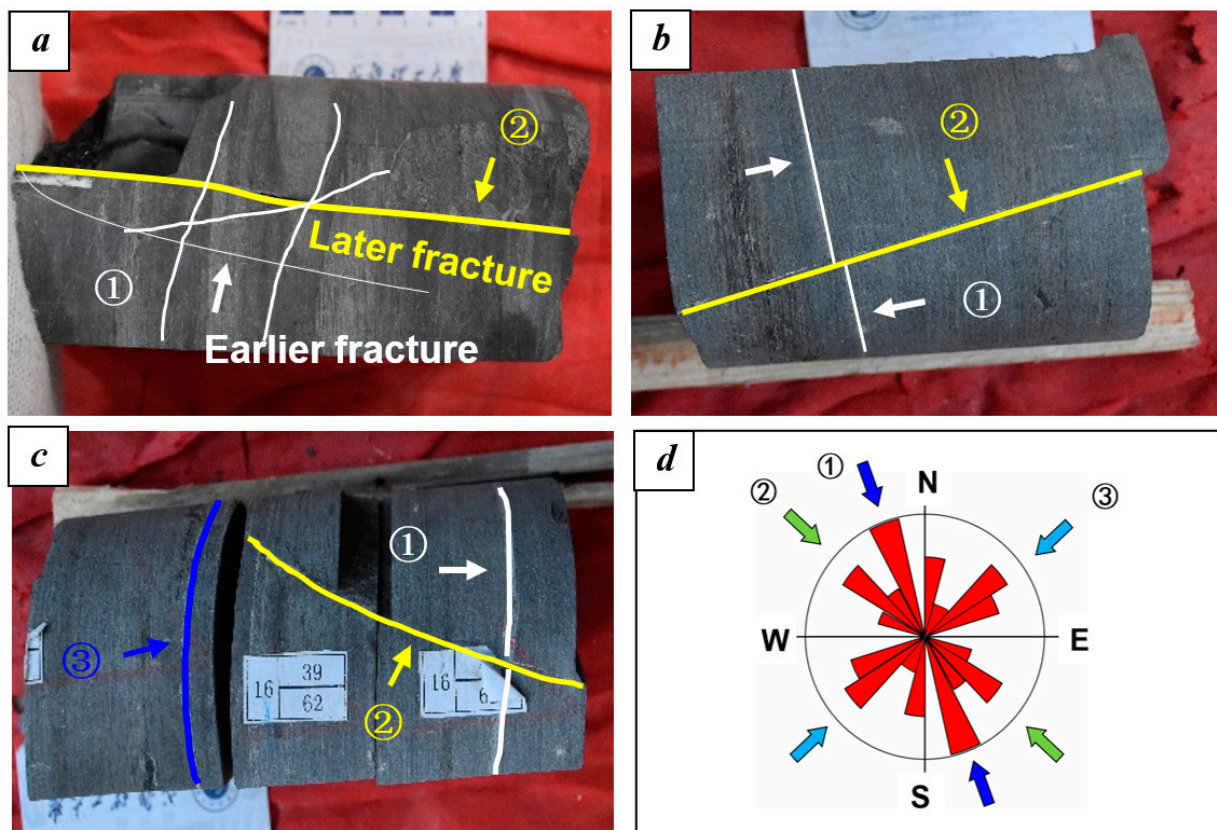


Figure 5. The drilling cores and rose map fracture strike and fracture period division of Fengcheng Formation in the Mahu Sag of the Junggar Basin. (a) Two sets or three sets of shear fractures, Well #6, 4744.48 m; (b) A late-formed high-angle tensile fracture intersecting with an early-formed bedding fracture, Well #3, 4705.03 m; (c) a late-formed shear fracture passing through an unfilled bedding fracture and an earlier-formed calcite-filled bedding fracture, Well #6, 4818.46 m; (d) Rose diagram of strikes of tectonic fractures in the Fengcheng Formation of the Mahu Sag. The numbers in the figure stand for the order of fractures generation.

Additionally, imaging logging results show that three sets of tectonic fractures developed in the Fengcheng Formation: NNW-SSE, NW-SE, and NE-SW. Among them, the development of NNW-SSE fractures is the most significant, followed by NW-SE and NE-SW fractures. These results based on imaging logging are highly consistent with the formation periods of fractures observed on the core (Figure 5d). Furthermore, imaging logging results indicate the development of three sets of tectonic fractures in the Fengcheng Formation, oriented NNW-SSE, NW-SE, and NE-SW. Among these, the NNW-SSE fractures exhibit the most significant development, followed by the NW-SE and NE-SW fractures. The results indicate that the formation periods of natural fractures, based on imaging logging, are consistent with those observed in the core samples.

Observation of microsections reveals the presence of microfractures in the Fengcheng Formation exhibiting multiple cutting phenomena. Figure 6a depicts the characteristics of hydraulic fractures at the microscopic scale, with fractures filled by multi-stage calcite.

Due to the recurring opening and closing of the fractures, the calcite crystals exhibit multi-stage growth characteristics. The initial calcite crystal growth is constrained, leading to the formation of tensile blocky-shaped calcite crystals. Subsequently, fractures expand, permitting unrestricted crystal growth. Moreover, an evident mutual cutting relationship exists between the fractures in the microsection shown in Figure 6b. Early calcite veins are intersected by thicker calcite veins that formed later (as illustrated in Figure 6b). Figure 6c illustrates three-stage veins, indicating that the fractures in the Fengcheng Formation have experienced a minimum of three stages. In summary, the microstructure of the Fengcheng Formation is highly intricate and displays characteristics indicative of multiple filling stages.

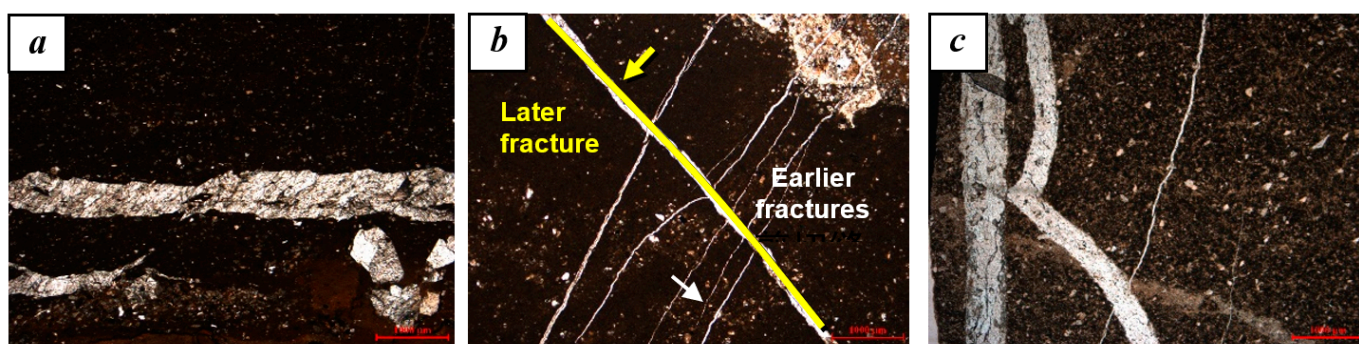


Figure 6. The microsections of Fengcheng Formation in the Mahu Sag of the Junggar Basin, showing the cutting relationship of natural fractures; (a) The hydraulic fractures at the microscopic scale with multi-stage calcite filling, Well #6, 4647.30 m; (b) Fractures with mutual cutting relationship, Well #3, 4699.40 m; (c) Three-stage veins, Well #3, 4609.97 m.

The observations of core and microsections reveal that the Fengcheng Formation shale of the Mahu Sag has developed at least three stages of fractures. The earliest fractures are mostly filled with horizontally fibrous calcite fractures. Mid-stage tectonic fractures, caused by tensional stress, are filled with blocky calcite. Finally, late-stage expansion fractures are primarily filled with blocky calcite and quartz. This indicates that the fractures developed within a relatively open expansion environment, leading to well-defined and regular features of the crystals.

4.3.2. Stable Carbon and Oxygen Isotope Analysis

Analyzing the stable carbon and oxygen isotope compositions of calcite fillings within fractures is a useful method for identifying different stages of fracture development and their associated diagenetic environments. Significant variations in the collected data or calculated formation temperatures could suggest the occurrence of distinct vein mineralization formation stages. In this study, twenty-one samples from the Fengcheng Formation of the Mahu Sag are applied to conduct the stable carbon and oxygen isotope analyses. Results demonstrate that $\delta^{18}\text{O}$ and $\delta^{13}\text{C}$ values of samples range from -10.17‰ to -3.43‰ , -15.76‰ and 4.10‰ , respectively. Figure 7 presents a negative correlation between $\delta^{18}\text{O}$ and $\delta^{13}\text{C}$ isotopes in the samples, suggesting that fracture developed across multiple stages. Based on the oxygen isotope thermometry equation proposed by Fritz and Simith (1970) [24], the paleotemperature of fracture formation can be calculated as follow:

$$T = 31.9 - 5.55 (\delta^{18}\text{O} - \delta^{18}\text{O}_w) + 0.7 (\delta^{18}\text{O} - \delta^{18}\text{O}_w)^2 \quad (1)$$

where, T is the paleotemperature at which filled calcite formed. $\delta^{18}\text{O}$ and $\delta^{18}\text{O}_w$ refers to the oxygen isotope value of the fracture filling and aqueous medium, respectively. In this study, the $\delta^{18}\text{O}_w$ equals to -0.5‰ according to the previous research [25].

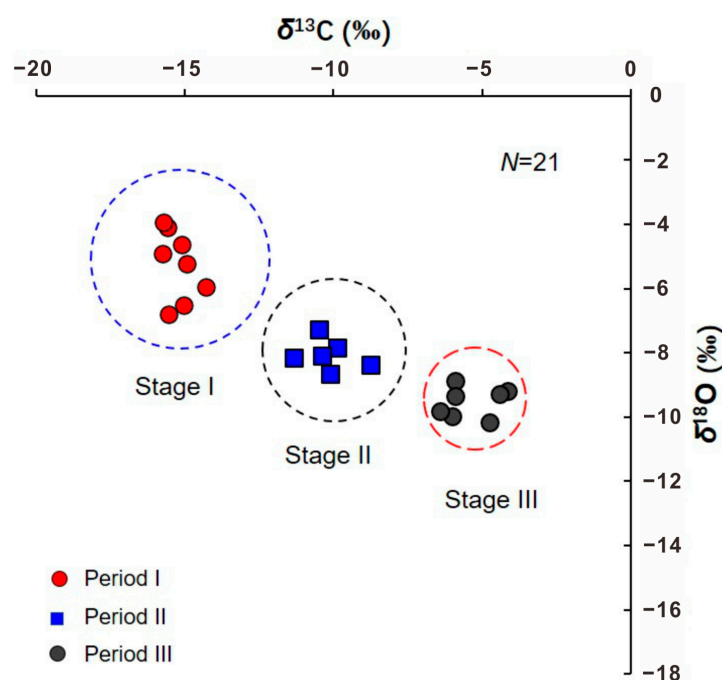


Figure 7. The relationship of $\delta^{18}\text{O}$ and $\delta^{13}\text{C}$ isotopes of fracture fillings in the Fengcheng Formation of the Mahu Sag.

Given an average ground temperature of 20 °C and a geothermal gradient of 2.65 °C/100 m in the Mahu Sag (Hu et al., 2020) [26], the burial depth at the time of fracture formation can be calculated. The distribution of $\delta^{13}\text{C}$ and $\delta^{18}\text{O}$ can be divided into three distinct stages. During the first stage of fractures, the $\delta^{18}\text{O}$ values of the fracture filling ranged from -3.93 to -6.76 ‰, with calculated temperatures between 70.22 °C and 109.09 °C, and corresponding burial depths of 1895.24 to 3361.82 m. Fibrous calcite was the primary filling material in these fractures. During the second stage of fractures, the fracture filling material had $\delta^{18}\text{O}$ values ranging from -7.32 to -8.02 ‰. This corresponds to calculated temperatures between 118.11 °C and 130.00 °C, and burial depths of 3702.18 to 4150.92 m. During the third stage of fractures, the $\delta^{18}\text{O}$ values of the filling material ranged from -8.28 to -9.07 ‰, with calculated temperatures between 134.59 °C and 149.12 °C, and corresponding burial depths of 4324.18 to 4872.56 m. The primary filling minerals in these fractures were blocky calcite and granular quartz. Therefore, based on the $\delta^{18}\text{O}$ values and temperature calculation results of the filling material in the fractures, we can conclude that the fracture formation can be divided into three stages, corresponding to different depths of burial: 1895.24–3361.82 m, 3702.18–4150.92 m, and 4324.18–4872.56 m.

4.3.3. Fluid Inclusion Tests

The paleotemperature during the time of entrapment can be determined by measuring the homogenization temperature of inclusions in fracture fillings, which assists in identifying the period of fracture formation (Li et al., 2023) [16]. In this study, inclusions were extracted from quartz and calcite that filled the tectonic fractures. The inclusion types primarily consisted of gas-liquid two-phase saline inclusions and hydrocarbon inclusions. Figure 8 indicates the morphologies of the inclusions in fracture fillings of the Fengcheng Formation in the Mahu Sag. The inclusions in quartz, size of 5–10 μm , are mainly irregular polygons with shape of sub-circular or spindle. In addition, the inclusions developed in the calcite fillings are densely distributed in groups or bands, exhibiting predominantly regular quadrilaterals and irregular polygons, with sizes ranging from 3–9 μm . Compared to quartz inclusions, calcite inclusions are more abundant but slightly smaller in size. Results reveal that the homogenization temperature of inclusions in the Fengcheng Formation can be roughly divided into three ranges (Figure 9). Table 1 summarizes the temperature and salin-

ities of the fluid inclusions in the Fengcheng Formation of Mahu Sag. Combined with core observations and microsection identification, it is inferred that the first stage of fractures is primarily filled with fibrous calcite, corresponding to temperature of 70–100 °C; the second stage of fractures are predominantly filled with elongated calcite crystals, corresponding to temperature of 110–130 °C; the third stage of fractures is mainly filled with quartz and calcite, along with some unfilled fractures. These fractures correspond to temperature of 130–150 °C.

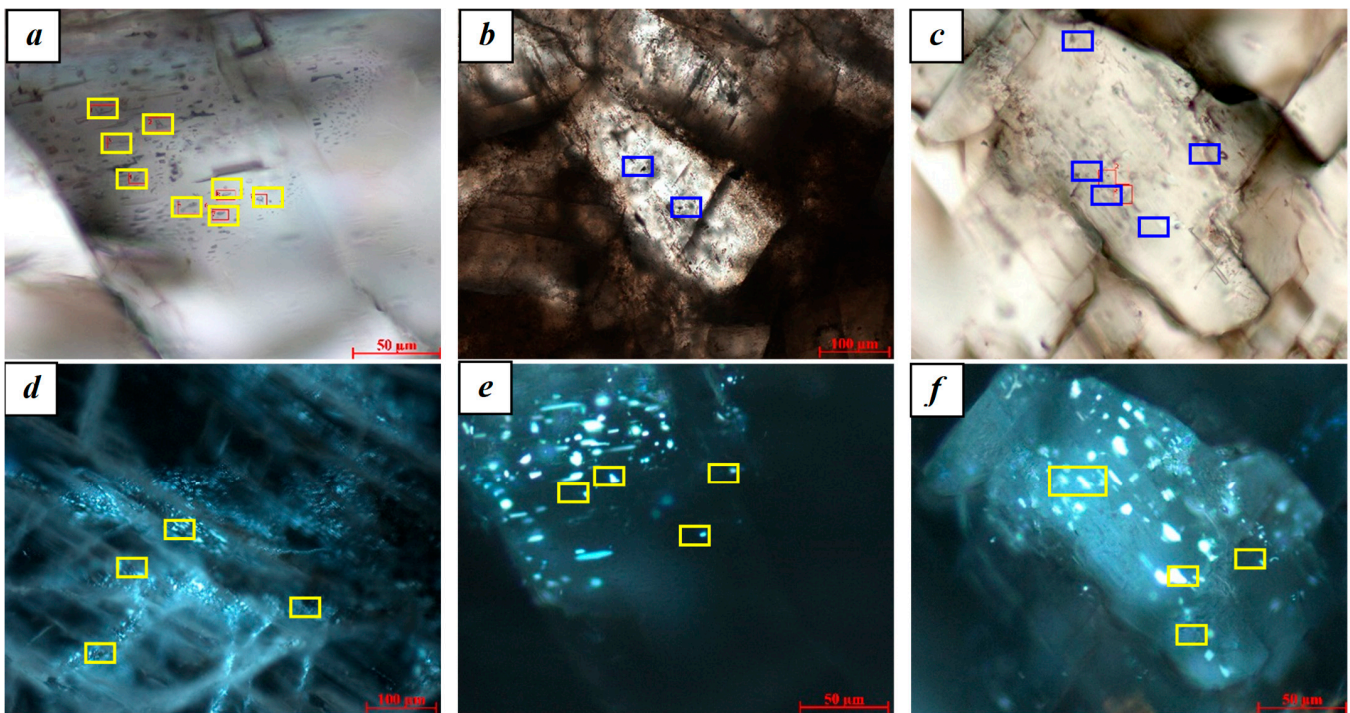


Figure 8. The fluid inclusion photos of Fengcheng Formation in the Mahu Sag of the Junggar Basin, showing the morphologies of the fluid inclusions; (a) X203, 4818.61 m, gas-liquid two-phase saline inclusions and hydrocarbon methane inclusions; (b) MY1, 4830.21 m, gas-liquid two-phase saline inclusions and hydrocarbon methane inclusions; (c) X203, 4812.35 m, gas-liquid two-phase saline inclusions and hydrocarbon methane inclusions; (d) X203, 4648.55 m, hydrocarbon methane inclusions; (e) X203, 4800.16 m, gas-liquid two-phase saline inclusions and hydrocarbon methane inclusions; (f) X203, 4812.35 m, gas-liquid two-phase saline inclusions and hydrocarbon methane inclusions.

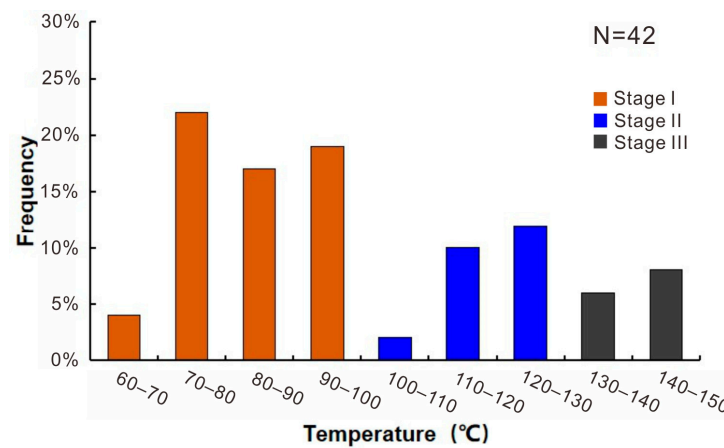


Figure 9. The distribution of the homogenization temperature of fluid inclusions in natural fracture fillings, the sample obtained from the Fengcheng Formation in the Mahu Sag of the Junggar Basin.

Table 1. The fluid inclusion test data of shale in the Fengcheng Formation of the Mahu Sag.

Well	Depth (m)	Inclusion Number	Size (μm)	Phase State	Homogenization Temperature ($^{\circ}\text{C}$)	Salinities (wt%)
X203	4818.61	1	8	Liquid phase	80	0.18
		2	6	Liquid phase	72	0.35
		3	7	Liquid phase	68	0.18
		4	6	Liquid phase	86	0.53
		5	5	Liquid phase	65	0.18
		6	3	Liquid phase	90	0.7
		7	3	Liquid phase	68	0.18
		8	4	Liquid phase	70	0.35

By examining the cutting relationships of fractures in the drilling cores, and micro-section, we have determined the sequence of tectonic fractures. Results suggest that there are at least three stages of natural fractures in the Fengcheng Formation of the Mahu Sag. These findings have significant implications for understanding the geology of the Mahu Sag and could be valuable for future exploration of natural resources or assessment of geological evolution in the region.

4.4. Genetic Mechanisms of Multiperiod Fractures

Figure 10 presents the burial history and thermal evolution profile for the Mahu Sag. Through a combination of multiple experiments, as well as an analysis of the burial history and evolution, the time frame for tectonic fracture formation can be ascertained. Results suggest that the geological tectonic evolution transpired during three distinct periods—243–266 Ma, 181–208 Ma, and 50–87 Ma—each playing a critical role in fostering the development of tectonic fractures within the Mahu Sag.

The initial stage of fracture evolution pertains to the Late Permian period (243–266 Ma), during which burial depths ranged from 1679 to 3056 m. The Mahu Sag in the Ordos Basin underwent NW-SE compression due to the collision between the Kazakhstan and Junggar plates. Consequently, these compressions led to the development of conjugate NWW-SEE and NNW-SSE shear fractures. The tectonic fractures that emerged during this stage exist in a relatively confined environment, inhibiting the growth of mineral crystals. These fractures are frequently filled with horizontally fibrous calcite. The fluid inclusions within the fracture fillings maintain a consistent temperature of 70–100 $^{\circ}\text{C}$.

The second stage of fracture evolution occurred during the Late Indosinian to Early Yanshanian period (181–208 Ma), with burial depths ranging from 3396 to 4151 m. Throughout the Mesozoic era, the Chinese mainland experienced compression and collision from the Pacific Plate and the Indian Plate, leading to a gradual uplift of the Mahu Sag. As a result of the westward subduction of the Pacific Plate towards the Eurasian Plate, conjugate NW-SE and NNW-SSE shear fractures can be formed in the Mahu Sag under the NNW-SSE stress. Most of the fractures formed during this period were filled with extensional calcite. These fractures existed in a semi-closed to semi-open environment, which constrained the growth of calcite crystals. Consequently, the calcite fillings within the fractures exhibited elongated and blocky appearances. The fluid inclusions in the calcite maintained a uniform temperature of 110–130 $^{\circ}\text{C}$.

The third stage of fracture development happened during the late Yanshanian to early Himalaya period (50–87 Ma) at depths ranging from 4528 to 4943 m. The movement and subduction of the Indian plate to the north had a distant effect on the central part of the Central Asian region, causing the Tarim Plate to move northward and resulting in compression in the near-SN direction across the studied area. This compression led to the formation of NNW-SSE and NNE-SSW strike-slip fractures, as well as associated faults near the primary faults. The fractures formed during this stage were mainly filled with

blocky calcite and quartz grains, with fluid inclusions exhibiting a uniform temperature of 130–150 °C.

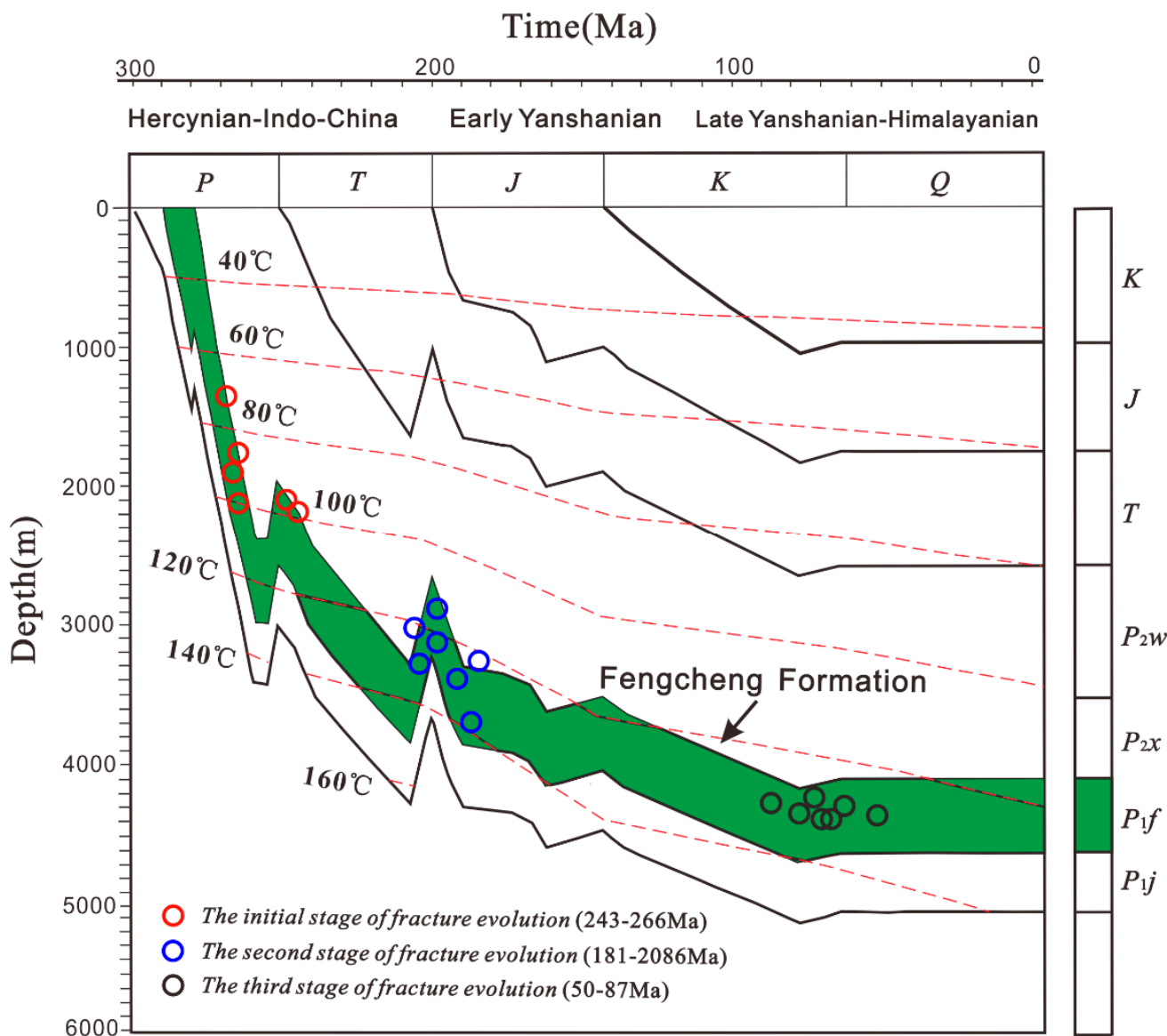


Figure 10. The burial history of Fengnan #4 Well and the estimated time-depth of different stages fractures in the Fengcheng Formation of the Mahu Sag.

4.5. Effect of Fractures on Oil Productivity

4.5.1. Microfractures

Microfractures contribute to the shale reservoir mainly by improving the storage space and enhancing the reservoir properties. In this study, the FESEM technique and nano-CT test were applied to analyze the effect of microfractures on shale reservoir properties.

Figure 11 shows the three-dimensional pore structure of the shale sample, which is mainly composed of dissolved pores, organic pores, diagenetic microfractures, and hydrocarbon overpressure fractures. Figure 11a,b illustrate irregularly shaped inorganic and organic pores with strong heterogeneity, mostly in an isolated state. Figure 11c displays irregularly shaped and unconnected inorganic fractures developed in the shale. Figure 11d exhibits the distribution of organic fractures.

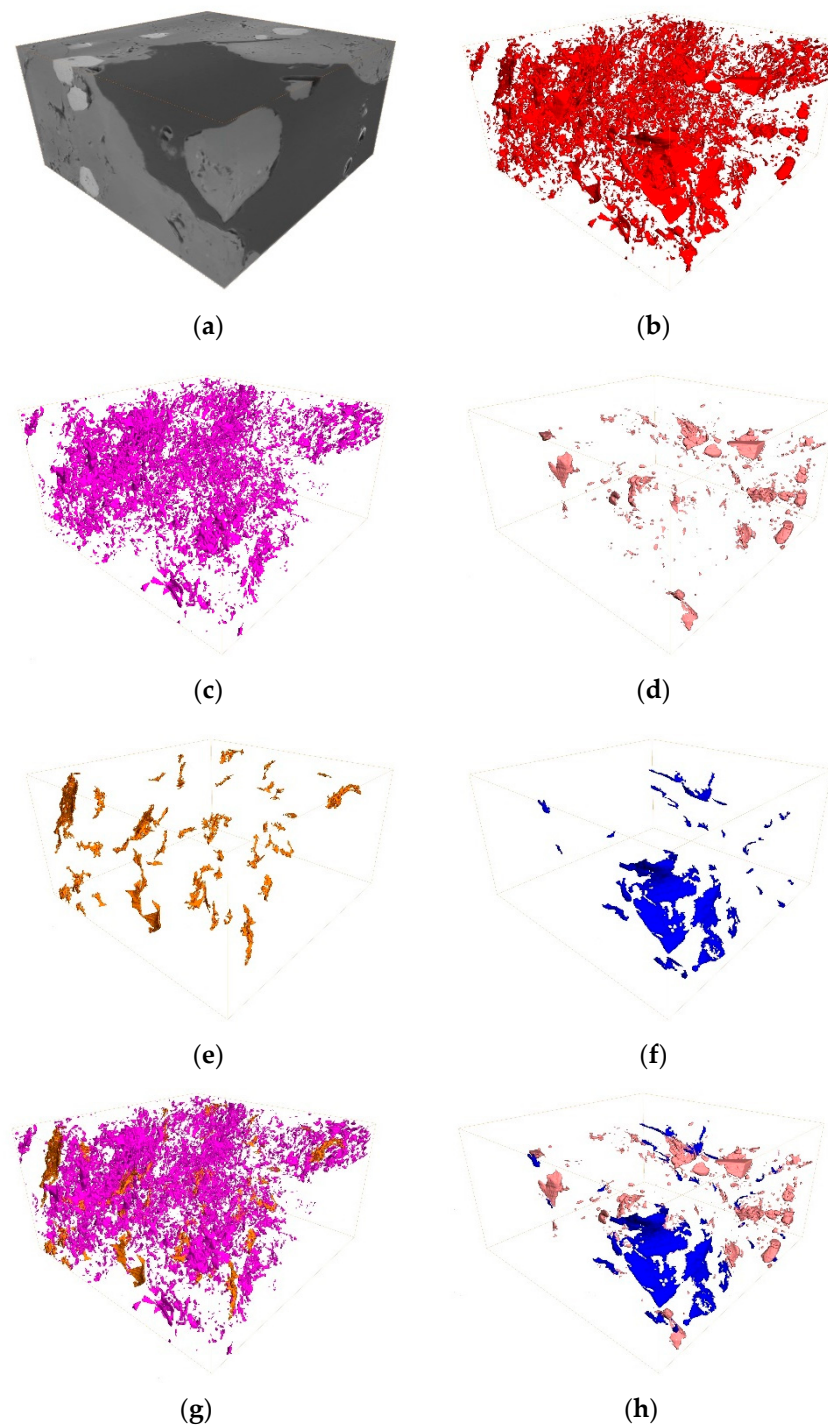
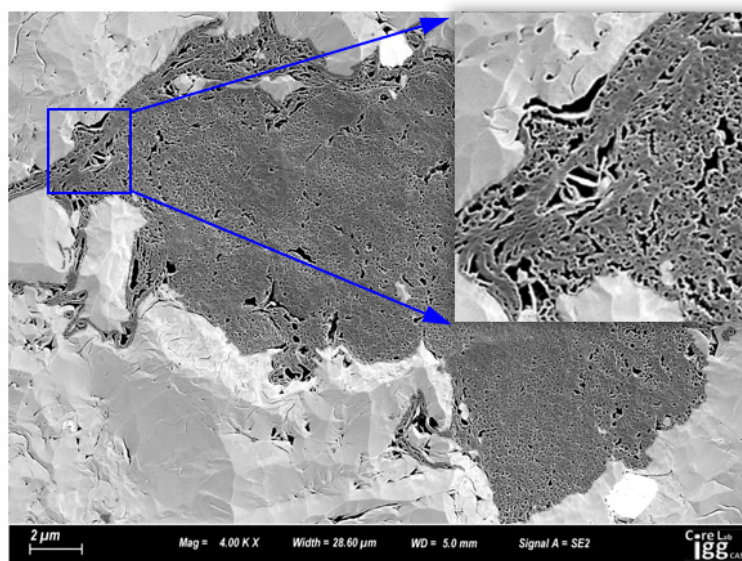


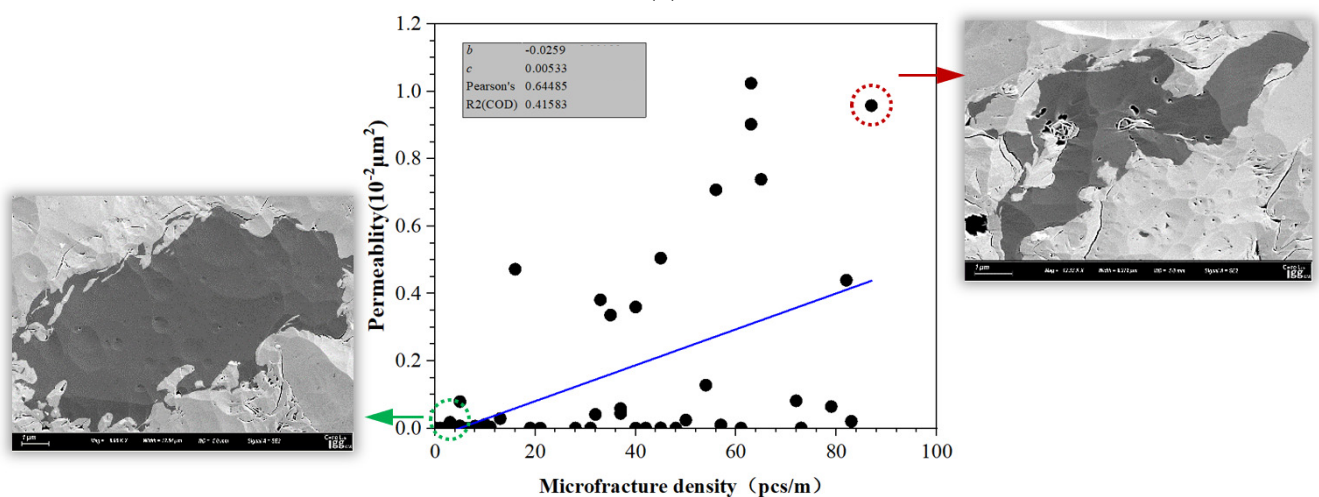
Figure 11. Nano-CT results of the shale sample, obtained from the Maye #1 Well in the Fengcheng Formation of the Mahu Sag; (a) 3D image of mineral composition; (b) 3D image of the volume of pores and fractures; (c) 3D image of the inorganic pores; (d) 3D image of the organic pores; (e) 3D image of the inorganic fractures; (f) 3D image of the organic fractures; (g) 3D image of the inorganic pores and fractures; (h) 3D image of the organic pores and fractures.

Figure 12a indicates the morphology and shape of the hydrocarbon overpressure microfractures in the Fengcheng Formation of the Mahu Sag. Combined with FE-SEM, it was proven that hydrocarbon overpressure microfractures, with small pore sizes and good connectivity, formed an effective permeability system. Hydrocarbon overpressure microfractures connect the isolated micropores in the shale reservoir, forming a connected pore space.

Figure 12b illustrates the relationship between the densities of hydrocarbon-generating overpressure microfractures and the permeabilities of the shale reservoir. The results reveal a positive correlation ($R^2 = 0.6448$) between the densities of hydrocarbon-generating overpressure microfractures and the permeabilities of the shale reservoir. Figure 12b left shows the SEM image of the shale reservoir in the study area for low permeability and overpressure microfractures density; Figure 12b right shows the SEM image of the shale reservoir in the study area for high permeability and overpressure microfractures density. As the densities of hydrocarbon-generating overpressure microfractures increase, permeabilities of the shale reservoir also increase. Consequently, hydrocarbon-generating overpressure microfractures enhance the effective storage capacity of the reservoir and optimize its pore structure [27]. Furthermore, the microfracture can establish a connection between the organic matter and the external flow channels, ultimately augmenting the reservoir's permeability.



(a)



(b)

Figure 12. (a) The morphology and shape of the hydrocarbon overpressure microfractures; (b) The relationship between the microfracture density and shale permeability in the Fengcheng Formation of the Mahu Sag.

4.5.2. Macrofractures

The location of high-yield and industrial gas flow wells predominantly near the fold belt highlights the significant impact of fracture development on natural gas production. In this study, twelve wells of the Fengcheng Formation in the Mahu Sag are investigated to analyze the development features of various fracture types based on imaging logging data. Figure 13a displays the intersection diagram of the fracture development index and the daily gas production of the twelve wells of the Fengcheng Formation in the Mahu Sag. Results indicate that the high-yield gas-bearing layers of the Fengcheng Formation exhibit well-developed fractures. To further examine the effect of the types of tectonic fractures on gas production, the associations between different types of tectonic fractures and daily gas production are plotted separately (Figure 13b–d). Results demonstrate that a positive correlation exists between daily gas production and the density of high-angle interlayer shear fractures, while the correlations with along-layer shear fractures and tensile fractures are not significant.

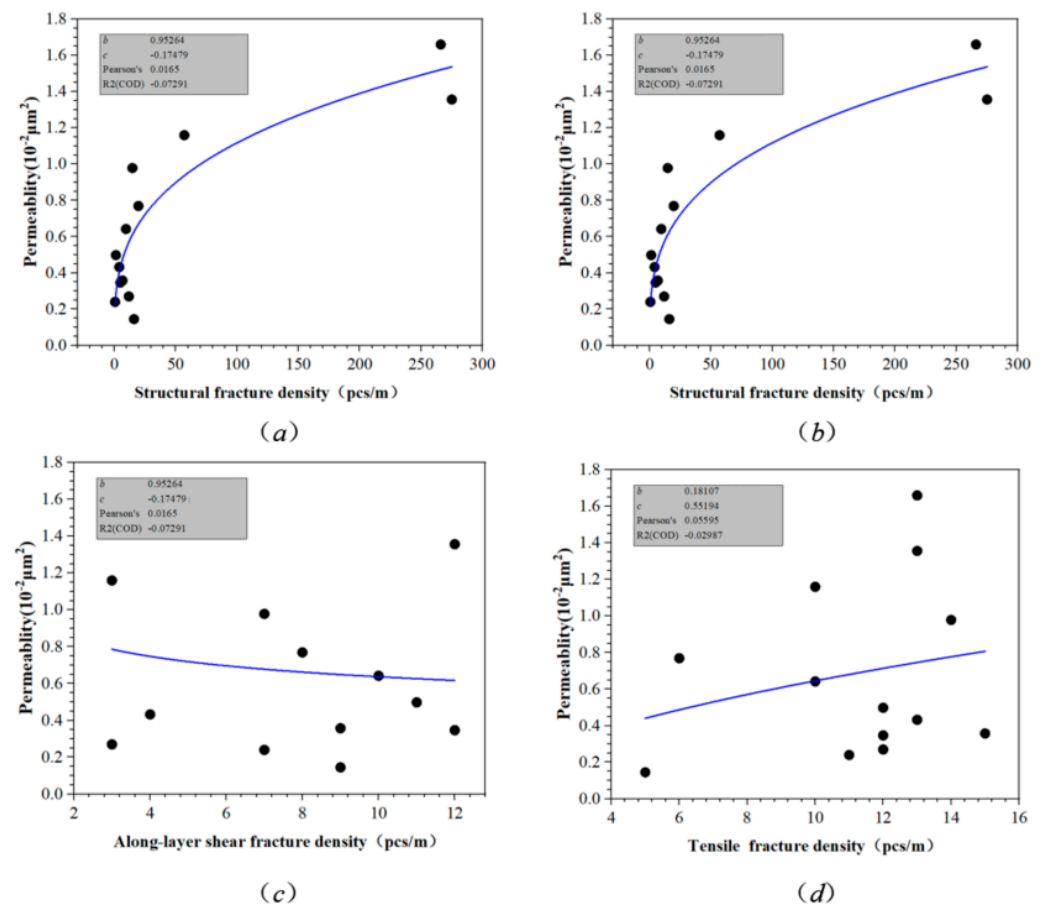


Figure 13. The relationships between the (a) tectonic fracture density, (b) high-angle interlayer shear fracture density, (c) along-layer shear fracture density, (d) tensile fracture density, and daily production in the Fengcheng Formation of the Mahu Sag.

The research findings hold considerable importance for natural gas exploration and development in the Mahu Sag. Based on these results, it is recommended that the development of high-angle interlayer shear fractures be prioritized during the exploration and development of high-yield gas-bearing layers. In addition, efforts should be intensified to study along-layer shear fractures and tensile fractures to gain a deeper understanding of their influence on gas production. Moreover, a comprehensive analysis should be undertaken, integrating imaging logging data with seismic data, to determine the characteristics of fractures and assess their impacts on natural gas production more precisely.

5. Conclusions

The fractures of the Fengcheng Formation in the Mahu Sag are analyzed by geological and geochemical methods. The conclusions are as follows:

- The Fengcheng Formation of the Mahu Sag contains two types of natural fractures: tectonic fractures and atectonic fractures. Tectonic fractures consist of high-angle interlayer shear fractures, along-layer shear fractures, and tensile fractures. Atectonic fractures include bedding fractures, hydraulic fractures, and hydrocarbon-generating overpressure fractures. The fractures are typically medium to high angle with filled minerals such as calcite and quartz. Additionally, shale with higher content of brittle minerals (quartz, feldspar, calcite and dolomite) is more susceptible to generating fractures. Vertically, fracture development is more prominent at the bottom of Feng #2 Formation and at the top of Feng #3 Formation.
- Combining the cutting relationships of natural fractures at both macro- and micro-scales, stable carbon and oxygen isotope analysis, and fluid inclusion results with the evolution of regional tectonic movements, the results suggest that the tectonic fractures in the study area can be classified into three stages. The first stage of fracture development occurred during the Late Permian period (243–266 Ma). The second stage of fracture evolution took place during the Late Indosinian to Early Yanshanian period (181–208 Ma). Finally, the third stage of fracture development occurred during the late Yanshanian to early Himalaya period (50–87 Ma).
- Among various types of tectonic fractures, the density of high-angle interlayer shear fractures has been found to exhibit a positive correlation with daily gas production, which suggests that high-angle interlayer shear fracture plays a significant role in promoting the production and transportation of hydrocarbon resources. Furthermore, hydrocarbon-generating overpressure microfractures, characterized by their small pore sizes and good connectivity, serve as an effective permeability system. This system connects previously isolated micropores in the shale reservoir, creating a connected pore space.

Author Contributions: X.X.: Writing—Review and Editing. W.W.: Review and Editing, Experiment, Writing—Review and Editing. C.L.: Data Curation. Z.W. and G.C.: Funding acquisition. F.C.: Review and Editing, Methodology, G.Z. and J.H.: Experiment, Data Curation. H.D. and K.L.: Investigation, Writing—Original Draft, Funding acquisition. All authors have read and agreed to the published version of the manuscript.

Funding: This research was funded by the Sichuan Province Science and Technology Plan Outstanding Youth Talent Project grant number [2020JDJQ0058].

Data Availability Statement: All the research data can be listed in the manuscript.

Conflicts of Interest: The authors declare no conflict of interest.

References

1. Zhao, W.; Hu, S.; Hou, L.; Yang, T.; Li, X.; Guo, B.; Yang, Z. Types and resource potential of continental shale oil in China and its boundary with tight oil. *Pet. Explor. Dev.* **2020**, *47*, 1–11. [[CrossRef](#)]
2. Jin, Z.; Zhu, R.; Liang, X.; Shen, Y. Several issues worthy of attention in current lacustrine shale oil exploration and development. *Pet. Explor. Dev.* **2021**, *48*, 1471–1484. [[CrossRef](#)]
3. Lu, G.; Zeng, L.; Dong, S.; Huang, L.; Liu, G.; Ostadhassan, M.; He, W.; Du, X.; Bao, C. Lithology identification using graph neural network in continental shale oil reservoirs: A case study in Mahu Sag, Junggar Basin, Western China. *Mar. Pet. Geol.* **2023**, *150*, 106168. [[CrossRef](#)]
4. He, W.J.; Qian, Y.X.; Zhao, Y.; Li, N.; Zhao, X.M.; Liu, G.L.; Miao, G. Exploration Implications of Total Petroleum System in Fengcheng Formation, Mahu Sag, Junggar Basin. *Xinjiang Pet. Geol.* **2021**, *42*, 641–655. (In Chinese) [[CrossRef](#)]
5. Tang, Y.; Cao, J.; He, W.-J.; Guo, X.-G.; Zhao, K.-B.; Li, W.-W. Discovery of shale oil in alkaline lacustrine basins: The late paleozoic Fengcheng Formation, Mahu sag, Junggar Basin, China. *Petrol. Sci.* **2021**, *18*, 1281–1293. [[CrossRef](#)]
6. Zhang, D.; Ranjith, P.G.; Perera, M.S.A. The brittleness indices used in rock mechanics and their application in shale hydraulic fracturing: A review. *J. Petrol. Sci. Eng.* **2016**, *143*, 158–170. [[CrossRef](#)]

7. Huo, J.; Wang, X.H.; Luo, C.; Huang, H.Y.; Chen, J.; Yin, C.; He, J.M. Fracture characteristics of Longmaxi shale in Southern Sichuan. *J. Eng. Geol.* **2021**, *29*, 171–182. [[CrossRef](#)]
8. Gale, J.F.W.; Reed, R.M.; Holder, J. Natural fractures in the Barnett Shale and their importance for hydraulic fracture treatments. *AAPG Bull.* **2007**, *91*, 603–622. [[CrossRef](#)]
9. Yang, Z.; Wang, X.; Ge, H.; Zhu, J.; Wen, Y. Study on evaluation method of fracture forming ability of shale oil reservoirs in Fengcheng Formation, Mahu sag. *J. Petrol. Sci. Eng.* **2022**, *215*, 110576. [[CrossRef](#)]
10. Zeng, L.; Su, H.; Tang, X.; Peng, Y.; Gong, L. Fractured tight sandstone oil and gas reservoirs: A new play type in the Dongpu depression, Bohai Bay Basin, China. *AAPG Bull.* **2013**, *97*, 363–377. [[CrossRef](#)]
11. Lyu, W.; Zeng, L.; Zhou, S.; Du, X.; Xia, D.; Liu, G.; Li, J.; Weng, J. Natural fractures in tight-oil sandstones: A case study of the Upper Triassic Yanchang Formation in the southwestern Ordos Basin, China. *AAPG Bull.* **2019**, *103*, 2343–2367. [[CrossRef](#)]
12. Liu, J.; Ding, W.; Yang, H.; Liu, Y. Quantitative Multiparameter Prediction of Fractured Tight Sandstone Reservoirs: A Case Study of the Yanchang Formation of the Ordos Basin, Central China. *SPE J.* **2021**, *26*, 3342–3373. [[CrossRef](#)]
13. Zhi, D.; Tang, Y.; He, W.; Guo, X.; Zheng, M.; Huang, L. Orderly coexistence and accumulation models of conventional and unconventional hydrocarbons in Lower Permian Fengcheng Formation, Mahu sag, Junggar Basin. *Pet. Explor. Dev.* **2021**, *48*, 43–59. [[CrossRef](#)]
14. Zou, C.; Yang, Z.; Cui, J.; Zhu, R.; Hou, L.; Tao, S.; Yuan, X.; Wu, S.; Lin, S.; Wang, L.; et al. Formation mechanism, geological characteristics and development strategy of nonmarine shale oil in China. *Pet. Explor. Dev.* **2013**, *40*, 15–27. [[CrossRef](#)]
15. Xie, X.; Deng, H.; Fu, M.; Hu, L.; He, J. Evaluation of pore structure characteristics of four types of continental shales with the aid of low-pressure nitrogen adsorption and an improved FE-SEM technique in Ordos Basin, China. *J. Petro. Sci. Eng.* **2021**, *197*, 108018. [[CrossRef](#)]
16. Li, X.Y.; Du, W.; Feng, X.; Shi, F.L.; Chen, Y.; Wang, Y.S.; Jiang, Z.X.; Luo, Q. Pressure Evolution Mechanism of Marine Shale Reservoirs and Shale Gas Accumulation Model: Evidence from Fluid Inclusions in the Wufeng–Longmaxi Formation in the Basin Margin Structural Transition Zone in Northern Guizhou Province, China. *Minerals* **2023**, *13*, 241. [[CrossRef](#)]
17. Gonzalez, L.A.; Lohmann, K.C. Carbon and oxygen isotopic composition of Holocene reefal carbonates. *Geology* **1985**, *13*, 811–814. [[CrossRef](#)]
18. Frezzotti, M.L.; Tecce, F.; Casagli, A. Raman spectroscopy for fluid inclusion analysis. *J. Geochem. Explor.* **2012**, *112*, 1–20. [[CrossRef](#)]
19. Aghli, G.; Moussavi-Harami, R.; Tokhmechi, B. Integration of sonic and resistivity conventional logs for identification of fracture parameters in the carbonate reservoirs: A case study, Carbonate Asmari Formation, Zagros Basin, SW Iran. *J. Petrol. Sci. Eng.* **2020**, *186*, 106728. [[CrossRef](#)]
20. Cao, J.; Xia, L.W.; Wang, T.T.; Zhi, D.M.; Tang, Y.; Li, W.W. An alkaline lake in the Late Paleozoic Ice Age (LPIA): A review and new insights into paleoenvironment and petroleum geology. *Earth-Sci. Rev.* **2019**, *202*, 103091. [[CrossRef](#)]
21. Song, T.; Huang, F.X.; Wang, S.Y.; Yang, F.; Lv, W.N.; Liu, C.; Jia, P.; Fan, J.J. Characteristics and exploration potential of Jurassic oil and gas reservoirs in Mahu sag of the Junggar Basin. *China Pet. Explor.* **2019**, *24*, 341–350. (In Chinese) [[CrossRef](#)]
22. Wang, J.T.; Yang, S.; Zou, Y.; Zhao, Y.; Huang, L.L.; Mou, L.W. Characteristics, genesis and distribution of high-quality reservoir of the first member of the Permian Fengcheng Formation in Mabei area, Junggar Basin. *China Pet. Explor.* **2022**, *27*, 99–109. (In Chinese) [[CrossRef](#)]
23. Zou, Y.; Qi, Y.P.; Song, D.; Chen, W.S.; Wei, P.Y. Geological characteristics and sweet spot evaluation of shale oil reservoir in Fengcheng Formation in Well Maye-1. *Xinjiang Pet. Geol.* **2022**, *43*, 714–723. (In Chinese) [[CrossRef](#)]
24. Fritz, P.; Smith, D.G.W. The isotopic composition of secondary dolomites. *Geochem. Cosmochim. Acta* **1970**, *34*, 1161–1173. [[CrossRef](#)]
25. Xia, Y.; Deng, H.C.; Wang, Y.Y.; He, J.H.; Xie, X.H.; Teng, J. Development characteristics and formation stages of natural fractures of the Triassic Leikoupo Formation in Pengzhou area of Western Sichuan Basin. *Mar. Orig. Pet. Geol.* **2021**, *26*, 81–89. (In Chinese) [[CrossRef](#)]
26. Hu, S.J.; Wang, X.J.; Cao, Z.L.; Li, J.Z.; Gong, D.Y.; Xu, Y. Formation conditions and exploration direction of large and medium gas reservoirs in the Junggar Basin, NW China. *Pet. Explor. Dev.* **2020**, *47*, 266–279. [[CrossRef](#)]
27. Xie, X.; Hu, L.; Deng, H.; Gao, J. Evolution of pore structure and fractal characteristics of marine shale during electromagnetic radiation. *PLoS ONE* **2020**, *15*, e0239662. [[CrossRef](#)]

Disclaimer/Publisher’s Note: The statements, opinions and data contained in all publications are solely those of the individual author(s) and contributor(s) and not of MDPI and/or the editor(s). MDPI and/or the editor(s) disclaim responsibility for any injury to people or property resulting from any ideas, methods, instructions or products referred to in the content.